Counteracting global warming by using a locally optimized solar radiation management

Davide Marchegiani[1] and Dietmar Dommenget[1]

[1]Monash University

November 26, 2022

Abstract

Solar Radiation Management (SRM) is regarded as a tool to potentially counteract global warming by increasing planetary albedo. Even though it has shown effective results in offsetting global surface temperature, one of its main limits lies in the persistence of major regional anomalies, for both surface temperature and precipitation. Here, using the Globally Resolved Energy Balance (GREB) model, we present experiments designed to completely offset global and regional surface temperature response due to CO2 forcing. Our innovative idea, is to employ a spatially and seasonally optimized SRM, as opposed to the state-of-the-art geoengineering which utilizes a homogeneous one. This approach allows to cut down surface warming by more than 99% in nearly all regions and seasons, with the exception of polar regions. This pilot study is opening up interesting pathways for further experiments with more complex models, to completely compensate global warming with SRM.

Counteracting global warming by using a locally optimized solar radiation management

D. Marchegiani[1], D. Dommenget[1]

[1]School of Earth, Atmosphere and Environment, ARC Centre of Excellence for Climate Extremes, Monash University, Clayton, Victoria, Australia.

Corresponding author: Davide Marchegiani (davide.marchegiani@monash.edu)

Key Points:

- Innovative spatially and seasonally optimized solar radiation management

- Regionally counteract the surface warming arising from increased greenhouse gases in the atmosphere

- Opening research pathways for better understanding the relationship between different atmospheric forcings and solar radiation management

Abstract

Solar Radiation Management (SRM) is regarded as a tool to potentially counteract global warming by increasing planetary albedo. Even though it has shown effective results in offsetting global surface temperature, one of its main limits lies in the persistence of major regional anomalies, for both surface temperature and precipitation. Here, using the Globally Resolved Energy Balance (GREB) model, we present experiments designed to completely offset global and regional surface temperature response due to CO_2 forcing. Our innovative idea, is to employ a spatially and seasonally optimized SRM, as opposed to the state-of-the-art geoengineering which utilizes a homogeneous one. This approach allows to cut down surface warming by more than 99% in nearly all regions and seasons, with the exception of polar regions. This pilot study is opening up interesting pathways for further experiments with more complex models, to completely compensate global warming with SRM.

1 Introduction

Solar Radiation Management (SRM) is one of the main branches of geoengineering, which proposes to counter the warming associated with increasing greenhouse gases (GHG) concentrations by reducing the amount of sunlight absorbed within the climate system [Royal Society, 2009]. Its main approach is to re-direct short-wave radiation back to space, by making the earth (either land/ocean surface or atmosphere) more reflective, so as to produce a cooling effect [Budyko, 1972; Crutzen, 2006]. Over the last few decades, SRM has gained ground among the scientific community, being regarded as a technique which could effectively counteract global warming [Jones et al., 2016; Tilmes et al., 2016]. In fact, geoengineering experiments included within the Geoengineering Model Intercomparison Project [Kravitz et al., 2011] framework, find robust mean surface temperature reduction when the total solar irradiance is reduced. For example, in recent years, some experiments have been designed which could effectively meet the 2 °C and 1.5 °C mean surface temperature warming targets set in the Paris Agreement [Muri et al., 2018; Tilmes et al., 2016, 2020]. However, these results come along with a relevant issue: although global SRM produces a negative radiative forcing that tends to cool the surface, it will inexorably fail to simultaneously offset temperature and precipitation changes in all regions [Andrews et al., 2010; Cambridge University Press, 2014; Ricke et al., 2010; Schmidt et al., 2012].

In fact, although the impact of SRM on the global mean temperature and precipitation is well understood in models, less understanding and agreement can be found for the spatial anomaly patterns [Kravitz et al., 2014; Ricke et al., 2010]. Indeed, despite the reduction of surface warming on a global average, conventional SRM still leaves regions with major surface temperature anomalies. Furthermore, reduction of incoming solar radiation could lead to undesirable effects, particularly on the hydrological cycle [Bala et al., 2010; Ricke et al., 2010; Robock et al., 2008]. We know that, as climate warms, the atmosphere tends to stabilize and the overall vertical motion weakens [Chou et al., 2010; Huang et al., 2013]. This decrease in vertical motion is partially generated directly by CO_2, which means that part of the precipitation response to climate change is independent of the surface warming [Gregory and Webb, 2008]. As a result, geo-engineering options aiming at weakening global warming without removing CO_2 from the atmosphere might fail to fully mitigate precipitation changes at global or regional scales [Bony et al., 2013].

In this paper, we use a series of simulation experiments with the Globally Resolved Energy Balance (GREB) Model to implement an innovative approach to SRM. Namely, we adopt a spatially and seasonally variable SRM, as opposed to its global and homogeneous most common

implementation. We investigate the response of surface temperature and precipitation, with a particular focus on seasonal and regional anomalies, in a scenario with double CO_2 and our localized SRM. This approach will illustrate what regional patterns of SRM would be required to fully compensate global warming in nearly all regions and seasons. Being mindful of the simplicity of our model, especially as far as the hydrological cycle is concerned, this study is meant to be seen as a pilot test to open up pathways for further development of similar techniques with more complex GCMs.

2 Methods

We carry out our analyses using the Globally Resolved Energy Balance (GREB) Model [Dommenget and Flöter, 2011; Stassen et al., 2019]. This is a simple global climate model, developed on a 3.75° x 3.75° horizontal latitude-longitude grid, consisting of 3 layers: land and ocean surface, atmosphere and deep ocean. The model simulates a variety of climate processes such as long-wave and short-wave radiation, heat transport in the atmosphere (both by isotropic diffusion and advection with the mean winds), the hydrological cycle (evaporation, precipitation and water vapour transport), a simple ice–snow albedo feedback and heat uptake in the subsurface ocean [Stassen et al., 2019]. The model is conceptually very different from Coupled General Circulation Models (CGCMs) as it assumes a mean, seasonally varying atmospheric circulation (reference climatology taken from the ERA-Interim 850 hPa level average from 1979 to 2015 [Dee et al., 2011]) and cloud cover (climatology taken from the ISCCP project [Rossow and Schiffer, 1991]) as boundary conditions. Subsequently, the model does not simulate internal (weather) fluctuations and a single year can be used to estimates its current mean state. It further uses flux correction to keep the model close to the observed climate [Dommenget and Flöter, 2011]. The main advantage of the GREB model for this study is the simplicity in which the cloud cover and albedo can be controlled.

We set up 6 different experiments, also listed in Table 1: (i) a control experiment, having default boundary conditions and a CO_2 concentration of 340ppm (the anomalies in this study are all computed with respect to this control run); (ii) 2xCO_2, having the same setting as the control run, but doubled CO_2 concentration (680ppm); (iii,iv) Homogeneous SRM, with the same setting as the 2xCO_2 experiment and, depending on the approach, either default short-wave radiation matrix (SWRM) or default cloud cover matrix (CLDM) scaled by a constant factor (so as to mimic the homogeneous SRM applications, imposing the same level of SRM everywhere. By construction, we forced the global mean surface temperature in these experiments to be equal to the control experiment. In order to achieve so, the factors used to scale the forcing pattern (FP) were 0.980 for the SWRM, and 1.093 for the CLDM, respectively); (v,vi) Localized SRM, similar to the Homogeneous one but following a spatially and seasonally variable SRM. All the experiments are set to be run for 50 years to near equilibrium and only the last year of the simulation is presented as the results.

In Ricke et al., 2010, it is assumed that SRM can be applied regionally and seasonally by controlling the effective albedo. Altering the cloud cover, for instance, could be one way of achieving this, but it needs to be considered that changes in the cloud cover would not only affect the albedo, but also the long wave radiation budget. For the local SRM experiments we present two alternative approaches: one in which we change the incoming short-wave radiaton regionally and seasonally, not specifying how this is being done (hereafter SRM$_{SW}$). In the second approach

we assume the cloud cover is altered regionally and seasonally to manage the short-wave radiation (hereafter SRM$_{CLD}$). For the localized SRM$_{SW}$ approach we deny the possibility for a location to reflect more sunlight than it receives, whereas for the SRM$_{CLD}$ approach the cloud cover can be either increased or decreased, provided it falls between 0 and 1. In order to achieve our localized SRM for both the SRM$_{SW}$ and SRM$_{CLD}$, we built up an iterative optimization scheme, so as to minimize local surface temperature anomalies. We start the iteration with a first guess FP and use it within a 30-years simulation along with the $2xCO_2$ forcing. In each following iteration we proportionally adjust the FP to the local mismatch between the control surface temperature ($\boldsymbol{T_{ctrl}}$) and the actual surface temperature resulting from the current iteration:

$$FP(x, y, t)^{i+1} = FP(x, y, t)^i + \Delta(x, y, t)^i \tag{1}$$

$$\Delta(x, y, t)^i = -\frac{\alpha}{S(x,y,t)} \cdot \left(T(x, y, t)^i - T_{ctrl}(x, y, t) \right) \tag{2}$$

where FP is a function of location $(\boldsymbol{x}, \boldsymbol{y})$ and time of the year $(\boldsymbol{t})$, $\boldsymbol{\alpha}$ is the learning rate of the optimization procedure, and S is a surface temperature sensitivity matrix used as a kernel for the artificial FP computation. For the results presented in this paper, $\boldsymbol{\alpha}$ is set to 0.34 for the SWRM and to 0.3 for the CLDM approach. More detailed instructions on the optimization procedure and the computation of S can be found in the supporting information.

3 Results

We conducted a series of $2xCO_2$ response experiments with and without SRM (see Methods and Table 1). Their annual mean surface temperature and precipitation responses are presented in Fig. 1 and the response in the seasonal cycle are shown in Fig. 2. The warming pattern for the $2xCO_2$ response experiments without SRM is similar to most CMIP models with increased warming over land, stronger warming at higher latitudes in winter times and a global mean warming of about 2.7 °C. The precipitation response also has some similarities with the CMIP models' response, but deviates from it due to having no regions of declined precipitation and an overall stronger

precipitation response. This deficiency is mostly related to the fact that the GREB model does not consider circulation changes [Stassen et al., 2019].

Table 1*. List of experiments carried out*

Name of the experiment	CO₂ concentration	SWRM forcing	CLDM forcing
Control	340 ppm	Default	Default
2xCO₂	680 ppm	Default	Default
Homogeneous SRM$_{SW}$	680 ppm	Scaled by 0.980	Default
Homogeneous SRM$_{CLD}$	680 ppm	Default	Scaled by 1.093
Localized SRM$_{SW}$	680 ppm	Optimization scheme for SWRM	Default
Localized SRM$_{CLD}$	680 ppm	Default	Optimization scheme for SWRM

In our first approach of SRM, we assume a globally homogeneous reduction in the solar constant to counteract the global mean warming, similarly to previous studies. By construction, the global mean warming with homogeneous SRM is essentially zero (Fig. 1b). However, it is interesting to notice how ineffective the homogeneous SRM can be on the regional scale. In fact, despite its ability to offset surface temperature on a global mean, homogeneous SRM still leaves major regional and seasonal anomalies for surface temperature. In particular, we find considerable overcompensation of the 2xCO₂ warming effect in the tropical and subtropical regions, leading to large-scale cooling in these areas (Fig. 1b). In turn, the higher latitudes 2xCO₂ warming effect is not fully compensated, leading to a significant warming. This mismatch between the homogeneous SRM and the 2xCO₂ response also projects onto the seasonal cycle, with the homogeneous SRM forcing being too weak in the cold (dark) season and too strong in the warm (bright) season in higher latitudes (Fig. 2b). The residual regional and seasonal warming and cooling of the surface temperature leads to regional changes in the precipitation as well. Regions and seasons with a warming response lead to increased precipitation and vice versa for cooling responses. The non-linearity in precipitation has a strong effect in the tropics, where an overall small global ranfall reduction can be witnessed. These results illustrate that the response pattern due to global 2xCO₂ forcing is different from that of altering the solar constant and, subsequently, a homogeneous SRM approach is bound to fail to compensate for 2xCO₂ forcing on a regional and seasonal scale. The differences on the regional and seasonal scale in surface temperature lead to global mean

differences in precipitation, since the precipitation response to changes in surface temperatures are not linear.
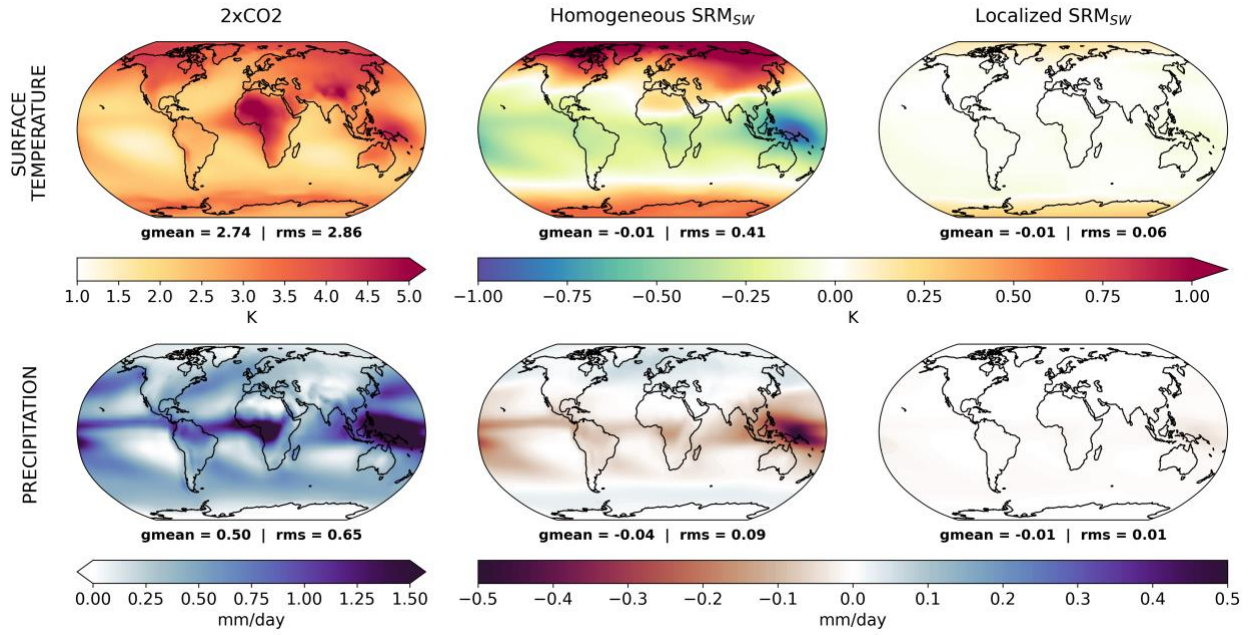

Figure 1. *Annual mean temperature (upper) and precipitation (lower) anomalies for the 2xCO₂ (left), Homogeneous SRM_SW (middle) and Localized SRM_SW experiments (right). The Homogeneous SRM_SW experiment is designed to have the same global mean (gmean) as the control. The area-weighted root mean square (rms) values based on all grid points are shown for each response pattern.*
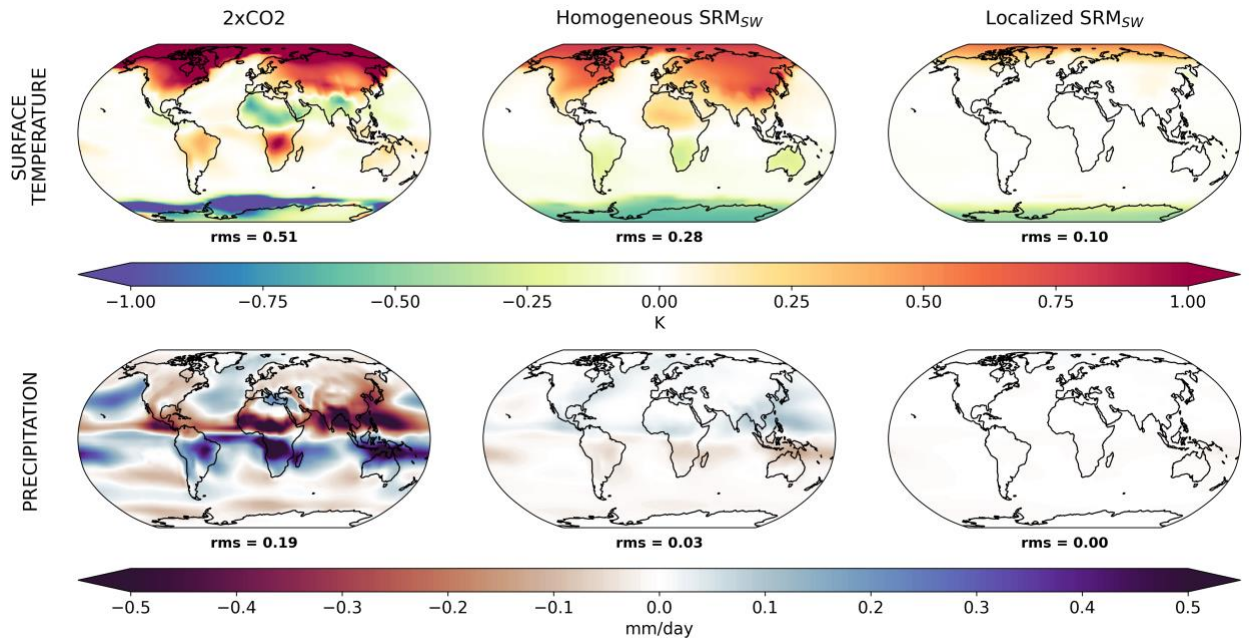

Figure 2. *Seasonal cycle, computed as $((DJF - JJA))/2$, of temperature (upper) and precipitation (lower) anomalies for the 2xCO₂ (left), Homogeneous SRM_SW (middle) and Localized SRM_SW experiments (right). The area-weighted root mean squared (rms) values based on all grid points are shown for each response pattern.*

As a consequence of the failure in the homogeneous SRM approach, one can consider to alter the SRM to a regional and seasonal approach. The local optimization scheme requires a first guess estimate of the sensitivity of the local surface temperature to the FP. Figure 3 shows the first guess sensitivity kernels for both the SRM$_{SW}$ and the SRM$_{CLD}$ approaches. These kernels reflect that the land regions are more sensitive to the local FP. In particular, for the cloud cover forcing we can notice a strong seasonal cycle at higher latitudes with a change of sign between the seasons. This reflects that the cloud cover is dominated by the short-wave albedo effect in summer, where there is strong incoming sun light, and it is dominated by the long wave warming effect in winter when there is no or little incoming sun light. However, it needs to be considered that the effective sensitivity to the FP in not just due to these local sensitivities, but will depend on the spatial structure of the FP as well. In a global forcing approach, the short-wave or cloud cover forcing will spatially synchronise and therefore strongly enhance the effective response.
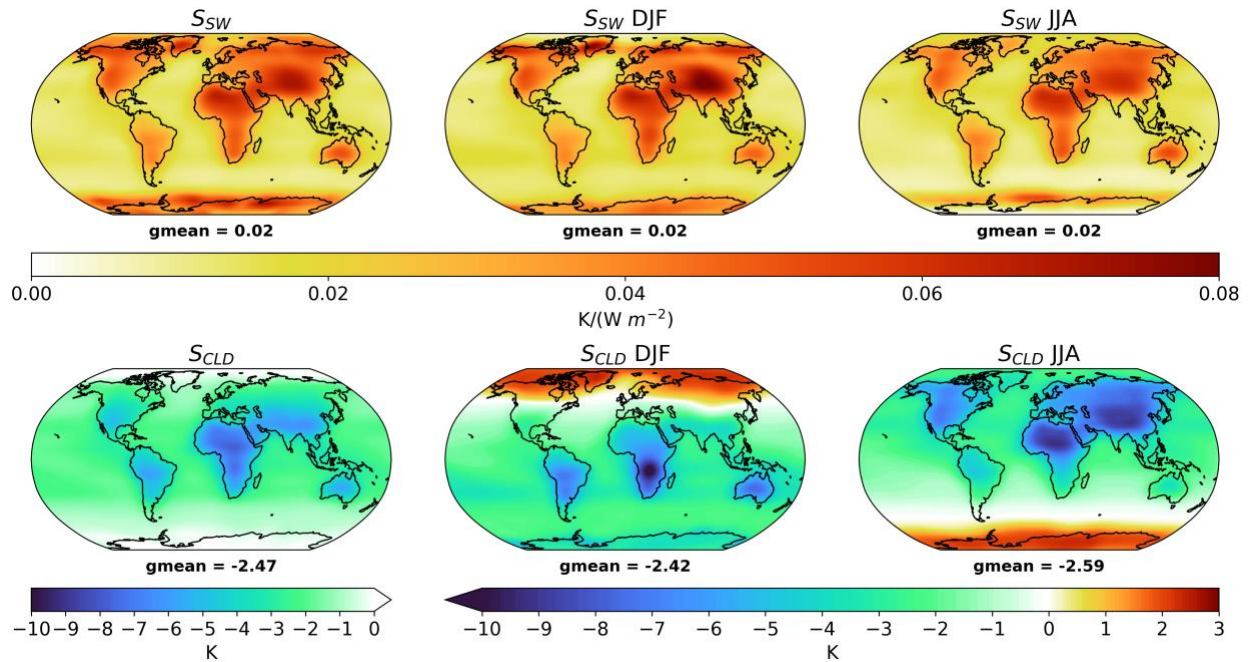

Figure 3. *Annual mean (left), and seasonal means DJF (middle) and JJA (right) for the Sensitivity matrix S$_{SW}$ (upper) and S$_{CLD}$ (lower). S$_{SW}$ (S$_{CLD}$) represents the change in surface temperature subsequent to a SW (CLD) change, and has been deployed as a kernel within the Localized SRM iteration procedure.*

The result of the iteration scheme finds the optimal local short-wave and cloud cover forcings needed to compensate the CO_2 forcing (see Fig. 4). It is worth noting that these can indeed compensate the CO_2 forcing almost completely for nearly all regions and seasons (see Figs. 1 and 2 for the SRM$_{SW}$ and SFigs. 1 and 2 for the SRM$_{CLD}$ approach). The SRM$_{SW}$ approach can compensate the annual mean response in surface temperature and precipitation locally much more effectively than the homogeneous SRM approach. Only in the polar regions we find some residual response. The annual cycle of the response is also largely reduced for most regions, but not in the polar regions.

The extent of our achievement can be further evidenced by taking the average over SREX Regions [Seneviratne et al., 2012] (SFig. 4). In fact, with our localized approach, we are able to maintain anomalies within ±0.1 °C for annual mean surface temperature and ±0.03 mm/day for

precipitation. By contrast, having a homogeneous implementation of SRM, leaves a lot of regions with fairly big regional anomalies, with values reaching up to 1 °C difference for surface temperature and 0.1 mm/day for precipitation. The SRM$_{CLD}$ approach is not quite as effective as the SRM$_{SW}$ approach, but it can still lead to a notably improved compensation of the CO_2 forcing in most regions, for both the annual mean and the seasonal cycle, in comparison to the homogeneous SRM approach (SFigs. 1, 2, 3, and 4). The local SRM$_{SW}$ approach would require a global mean increase in reflection of incoming sun light of about 7 W/m^2, with somewhat stronger amplitudes over land (Fig. 4). The SRM$_{SW}$ forcing does have strong seasonality at higher latitudes on both hemispheres. In both hemisphere we would require enhanced reflection of incoming sunlight in the cold seasons. In our approach, though, we deny the possibility for a location to reflect more sunlight than it receives (this can be witnessed by noticing how S$_{SW}$ doesn't have negative values and how Figs. 4a, 4b and 4c don't present negative anomalies). Thus, in the polar regions in winter we cannot reflect as much sun light as would be needed to compensate for the CO_2 forcing. Therefore, the optimized local SRM$_{SW}$ approach reflects more sun light at latitudes close to the polar regions, which still get enough sun light (at about 50o-60o N/S). For the SRM$_{CLD}$ approach, in which the cloud cover can be either increased or decreased (provided it falls between 0 and 1), we would require a global mean increase in cloud cover of about 6%. This would, however, have strong regional and seasonal differences. The largest changes in cloud cover would be up to 40% increase in midlatitudes' continental region of the Northern Hemisphere during winter, whereas there would be a consistent decrease in cloud cover over the poles' respective winters. The strong change in the midlatitudes would thus be needed also to counteract the CO_2 forcing poleward of these latitudes, since poleward cloud cover increase, in winter, would have no cooling effect due to missing sunlight.
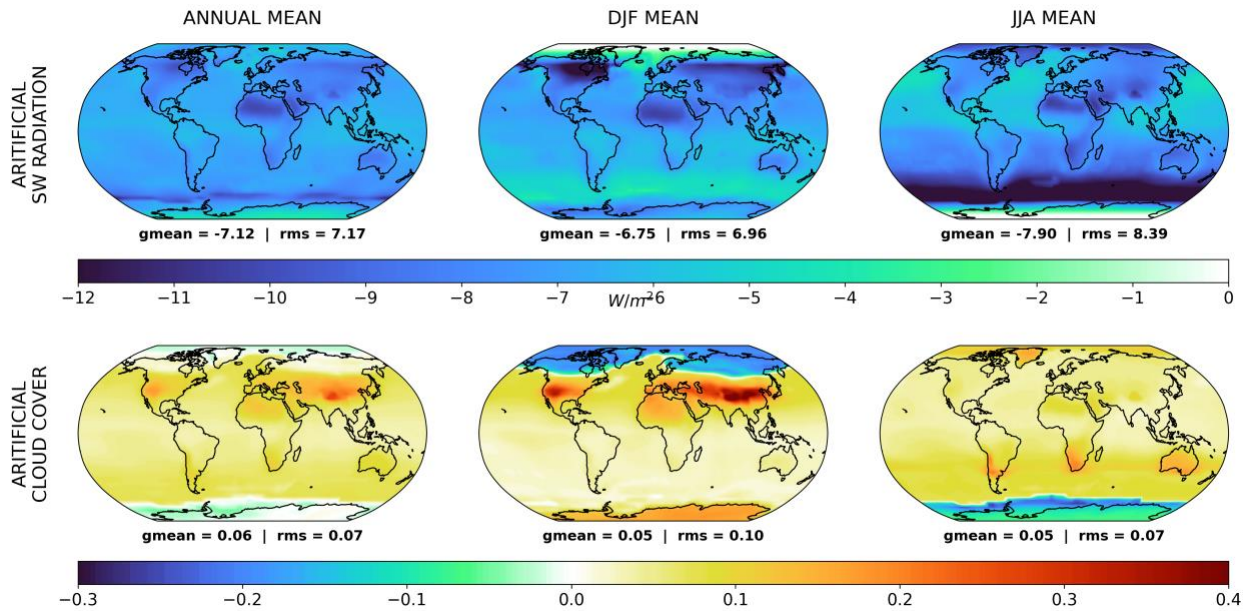

Figure 4. *The optimized, localised forcing patterns for SRM$_{SW}$ (upper) and SRM$_{CLD}$ (lower) for the annual mean (left), and seasonal means DJF (middle) and JJA (right).*

4 Summary and discussion

We used the simple GREB model as a pilot-test to assess a new approach to SRM, consisting of tailoring the amount of SRM applied to specific regions and seasons. Here we followed two approaches: controlling the effective albedo directly altering the incoming short-wave radiation, without specifying how this is done; or changing the cloud cover boundary condition. In both approaches we find that, by using the locally and seasonally optimized SRM methods, it would be possible to effectively counteract nearly all of the global and regional warming arising from increased GHG in the atmosphere. The only regions that would have significant residual warming would be the polar regions.

If we assume that such locally optimised SRM is mainly achieved by altering the cloud cover or cloud brightness [Christensen et al., 2020; Lu et al., 2018], then it would require up to 40% increase in cloud cover over some continental regions. These would be fairly substantial changes to the cloud cover and it is beyond this study to evaluated how such substantial changes could be achieved. This would require CGCM simulations in which clouds can artificially be controlled, while at the same time being also affected by the surrounding atmospheric conditions.

In the approach we followed here, it is implicitly assumed that local SRM does have primarily local effects. That is, you change SRM at one location and it only affects that area, without influencing other distant locations. This may be a good approximation, in particular over land, but will in general not be accurate. The fact that changes in SRM can have remote effects has two important consequences: first, in estimating what local changes in SRM are needed to counteract global warming in all regions, we also need to consider the non-local effect of SRM. The results of this study already give some indication of such non-local effects. For instance, the polar regions have largely been controlled by SRM in lower latitudes (see. Fig. 4) although we did not explicitly design the approach to achieve this. Secondly, the non-local effect of SRM could be used to control global warming in regions where SRM may not be possible or hard to achieve. For instance, it may be possible to only control SRM over oceanic regions and thereby indirectly controlling also the warming over land. This would potentially be possible, as much of the land warming is indeed controlled by the ocean warming [Cess et al., 1990; Dommenget, 2009].

The precipitation response in SRM experiments is of particular interest, as previous studies have found that while surface warming can be counteracted on the global mean, the precipitation would still change substantially [Bala et al., 2008, 2010; Ricke et al., 2010; Robock et al., 2008]. In our GREB model experiments, we managed to efficiently control both at the same time. However, this result should be taken with caution, as the GREB model does not consider any atmospheric circulation changes but the latter are central for understanding precipitation changes [Stassen et al., 2019; Yang et al., 2018]. Indeed, one of the main aspects of precipitation changes during global warming is the globally muted response of about 2% increase per degree global warming, rather than the 7% expected from the atmospheric humidity increase. Such muted response can only be explained by a weakening of the tropical circulation. These aspects are not simulated in the GREB model and would require further studies with fully complex CGCMs.

A key aspect in understanding how you could counteract CO_2 forcing with SRM is to understand how the two different forcing differ in their spatial and seasonal pattern. In the GREB model we essentially only consider the horizonal and seasonal differences, but neglect any differences in the

vertical structure of these two forcings. However, the CO_2 and SRM forcing do have substantial difference in the vertical structure, which are likely to affect the atmospheric circulation and subsequently the precipitation. Further studies with CGCMs need to address how these differences would affect SRM approaches. In summary, our experiments can be seen as a useful starting point to build a theoretical framework for understanding how locally and seasonally optimized SRM can counteract global warming. These should be used to motivate further studies with CGCM simulations to address this problem.

Acknowledgments

Data availability statement

Simulation outputs used in this work are available for download here: (https://doi.org/10.26180/15128088)

References

Royal Society (Great Britain). Geoengineering the climate : science, governance and uncertainty. (Royal Society, 2009).

Crutzen, P. J. Albedo Enhancement by Stratospheric Sulfur Injections: A Contribution to Resolve a Policy Dilemma? Climatic Change 77, (2006).

Budyko, M. I. The future climate. Eos, Transactions American Geophysical Union 53, (1972).

Jones, A. C., Haywood, J. M. & Jones, A. Climatic impacts of stratospheric geoengineering with sulfate, black carbon and titania injection. Atmospheric Chemistry and Physics 16, (2016).

Tilmes, S., Sanderson, B. M. & O'Neill, B. C. Climate impacts of geoengineering in a delayed mitigation scenario. Geophysical Research Letters 43, 8222–8229 (2016).

Kravitz, B. et al. The Geoengineering Model Intercomparison Project (GeoMIP). Atmospheric Science Letters 12, (2011).

Muri, H. et al. Climate Response to Aerosol Geoengineering: A Multimethod Comparison. Journal of Climate 31, (2018).

Tilmes, S. et al. Reaching 1.5 and 2.0 °C global surface temperature targets using stratospheric aerosol geoengineering. Earth System Dynamics 11, (2020).

Andrews, T., Forster, P. M., Boucher, O., Bellouin, N. & Jones, A. Precipitation, radiative forcing and global temperature change. Geophysical Research Letters 37, (2010).

Ricke, K. L., Morgan, M. G. & Allen, M. R. Regional climate response to solar-radiation management. Nature Geoscience 3, 537–541 (2010).

Schmidt, H. et al. Solar irradiance reduction to counteract radiative forcing from a quadrupling of CO.sub.2: climate responses simulated by four earth system models. Earth System Dynamics 3, 63–78 (2012).

Climate Change 2013 - The Physical Science Basis. (Cambridge University Press, 2014). doi:10.1017/CBO9781107415324.

Kravitz, B. et al. A multi-model assessment of regional climate disparities caused by solar geoengineering. Environmental Research Letters 9, (2014).

Robock, A., Oman, L. & Stenchikov, G. L. Regional climate responses to geoengineering with tropical and Arctic SO2 injections. Journal of Geophysical Research 113, (2008).

Bala, G., Caldeira, K. & Nemani, R. Fast versus slow response in climate change: implications for the global hydrological cycle. Climate Dynamics 35, (2010).

Chou, C. & Chen, C.-A. Depth of Convection and the Weakening of Tropical Circulation in Global Warming. Journal of Climate 23, (2010).

Huang, X. et al. A Radiative–Convective Equilibrium Perspective of Weakening of the Tropical Walker Circulation in Response to Global Warming. Journal of Climate 26, (2013).

Gregory, J. & Webb, M. Tropospheric Adjustment Induces a Cloud Component in CO2 Forcing. Journal of Climate 21, (2008).

Bony, S. et al. Robust direct effect of carbon dioxide on tropical circulation and regional precipitation. Nature Geoscience 6, 447–451 (2013).

Stassen, C., Dommenget, D. & Loveday, N. A hydrological cycle model for the Globally Resolved Energy Balance (GREB) model v1.0. Geoscientific Model Development 12, 425–440 (2019).

Seneviratne, S. I. et al. Changes in Climate Extremes and their Impacts on the Natural Physical Environment. in Managing the Risks of Extreme Events and Disasters to Advance Climate Change Adaptation (eds. Field, C. B., Barros, V., Stocker, T. F. & Dahe, Q.) (Cambridge University Press). doi:10.1017/CBO9781139177245.006.

Christensen, M. W., Jones, W. K. & Stier, P. Aerosols enhance cloud lifetime and brightness along the stratus-to-cumulus transition. Proceedings of the National Academy of Sciences 117, (2020).

Lu, Z. et al. Biomass smoke from southern Africa can significantly enhance the brightness of stratocumulus over the southeastern Atlantic Ocean. Proceedings of the National Academy of Sciences 115, (2018).

Dommenget, D. The Ocean's Role in Continental Climate Variability and Change. Journal of Climate 22, (2009).

Cess, R. D. et al. Intercomparison and interpretation of climate feedback processes in 19 atmospheric general circulation models. Journal of Geophysical Research 95, (1990).

Bala, G., Duffy, P. B. & Taylor, K. E. Impact of geoengineering schemes on the global hydrological cycle. PNAS vol. 105 (2008).

Yang, M., Zhang, G. J. & Sun, D.-Z. Precipitation and Moisture in Four Leading CMIP5 Models: Biases across Large-Scale Circulation Regimes and Their Attribution to Dynamic and Thermodynamic Factors. Journal of Climate 31, (2018).

Dommenget, D. & Flöter, J. Conceptual understanding of climate change with a globally resolved energy balance model. Climate Dynamics 37, 2143–2165 (2011).

Dee, D. P. et al. The ERA-Interim reanalysis: configuration and performance of the data assimilation system. Quarterly Journal of the Royal Meteorological Society 137, (2011).

Rossow, W. B. & Schiffer, R. A. ISCCP Cloud Data Products. Bulletin of the American Meteorological Society 72, (1991).

Counteracting global warming by using a locally optimized solar radiation management

D. Marchegiani[1], D. Dommenget[1]

[1]School of Earth, Atmosphere and Environment, ARC Centre of Excellence for Climate Extremes, Monash University, Clayton, Victoria, Australia.

Corresponding author: Davide Marchegiani (davide.marchegiani@monash.edu)

Supporting information content
1.Supplementary methods
2.Supplementary figures

1.Supplementary methods

Within our localized SRM approach, we built up an iterative optimization scheme in order to minimize local surface temperature anomalies (see Methods). The total number of iterations carried out for the FP optimization was 20. As a diagnostic to assess the degree of optimization, we used the root mean square error (rms) estimated for every grid point, between the annual mean of the i-th iteration and the control run, for both surface temperature and precipitation, respectively. In general, the scheme started converging around the 4th-5th iteration. However, minor variations were still present after convergence so, for the analyses shown, we chose the iteration with the minimum rms value among all 20 iterations. These turned out to be the 5th iteration for the SRM_{SW} approach and the 16th iteration for the SRM_{CLD} approach.

One of the core steps of our optimized procedure has been that of creating a kernel which could enable us to quantify, within our model, the sensitivity of surface temperature to changes in the FP. In order to obtain this sensitivity matrix S, we developed a series of perturbation experiments with the following setup: we carried out a 30-years $2xCO_2$ run, in which we scaled the FP along a ($15° \times 15°$) moving square, and estimated S* at this location by the change in surface temperature:

$$S^*(x,y,t_S) = \frac{\Delta T(x,y,t_S)}{\Delta FP(x,y,t_S)} = \frac{T(x,y,t_S)_\delta - T(x,y,t_S)_{ctrl}}{FP(x,y,t_S)_\delta - FP(x,y,t_S)_{ctrl}} \qquad (3)$$

with the surface temperature of the perturbation experiments, T_δ, the control, T_{ctrl}, the FP of the perturbation experiments, FP_δ, and the control, FP_{ctrl}. We repeated this for all locations and for each season (t_S) separately, for a total of 800 experiments. The final S is obtained by first joining all the S* together, smoothing them with a gaussian filter applied along the spatial coordinates, and ultimately by performing a linear interpolation over time.
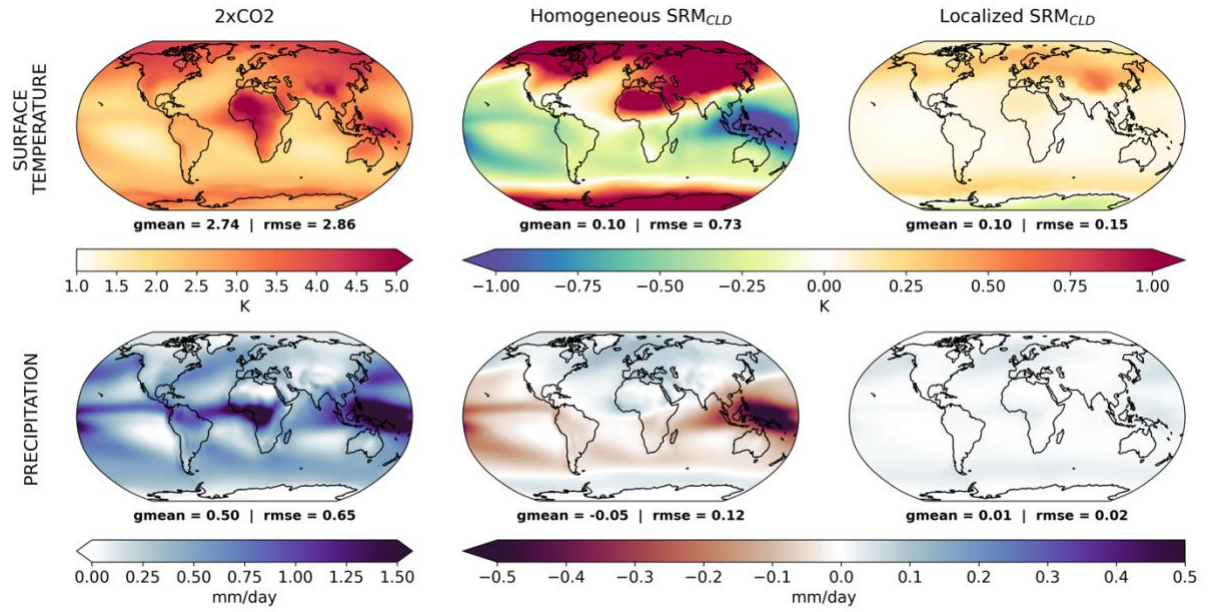
2.Supplementary Figures

Supplementary Figure 1. Annual mean temperature (upper) and precipitation (lower) anomalies for the $2xCO_2$ (left), Homogeneous SRM_{CLD} (middle) and Localized SRM_{CLD} experiments (right). The Homogeneous SRM_{CLD} experiment is designed to have the same global mean (gmean) as the control. The area-weighted root mean square (rms) values based on all grid points are shown for each response pattern.
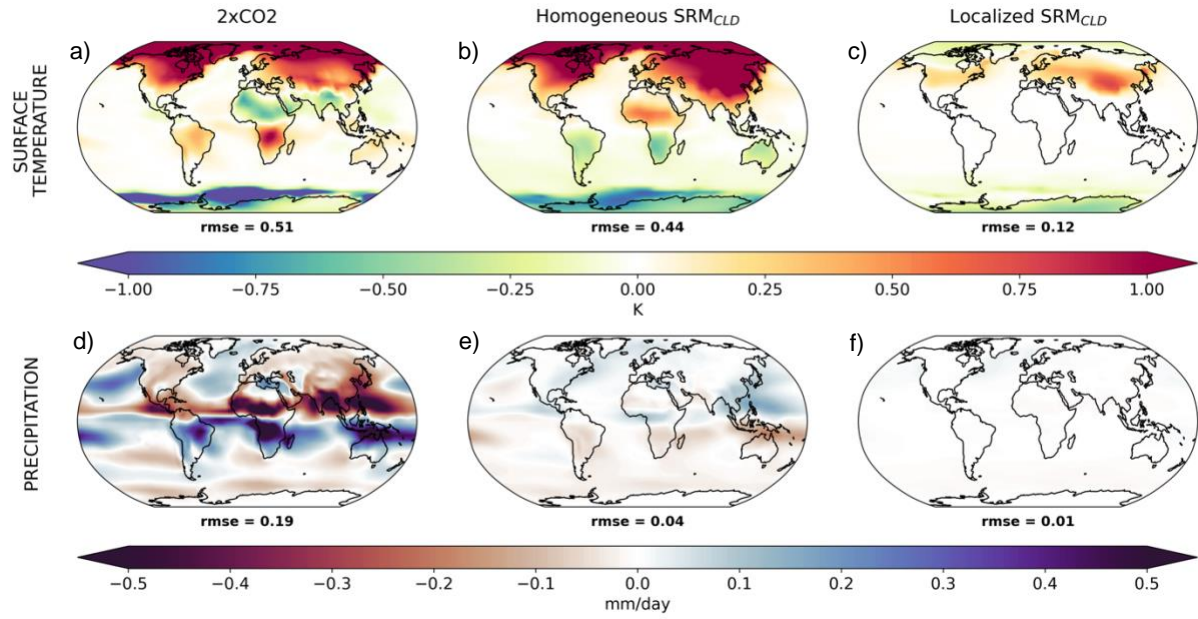
Supplementary Figure 2. Seasonal cycle, computed as $(DJF - JJA)/2$, of temperature (upper) and precipitation (lower) anomalies for the $2xCO_2$ (left), Homogeneous SRM_{CLD} (middle) and Localized SRM_{CLD} experiments (right). The area- weighted root mean squared (rms) values based on all grid points are shown for each response pattern.

Supplementary Figure 3. Annual mean anomalies over SREX regions [Seneviratne et al., 2012] of temperature (upper) and precipitation (lower), for the $2xCO_2$ (black circle), Homogeneous SRM_{SW} (red square), Homogeneous SRM_{CLD} (blue square), Localized SRM_{SW} (red cross) and Localized SRM_{CLD} (blue cross) experiments, respectively.
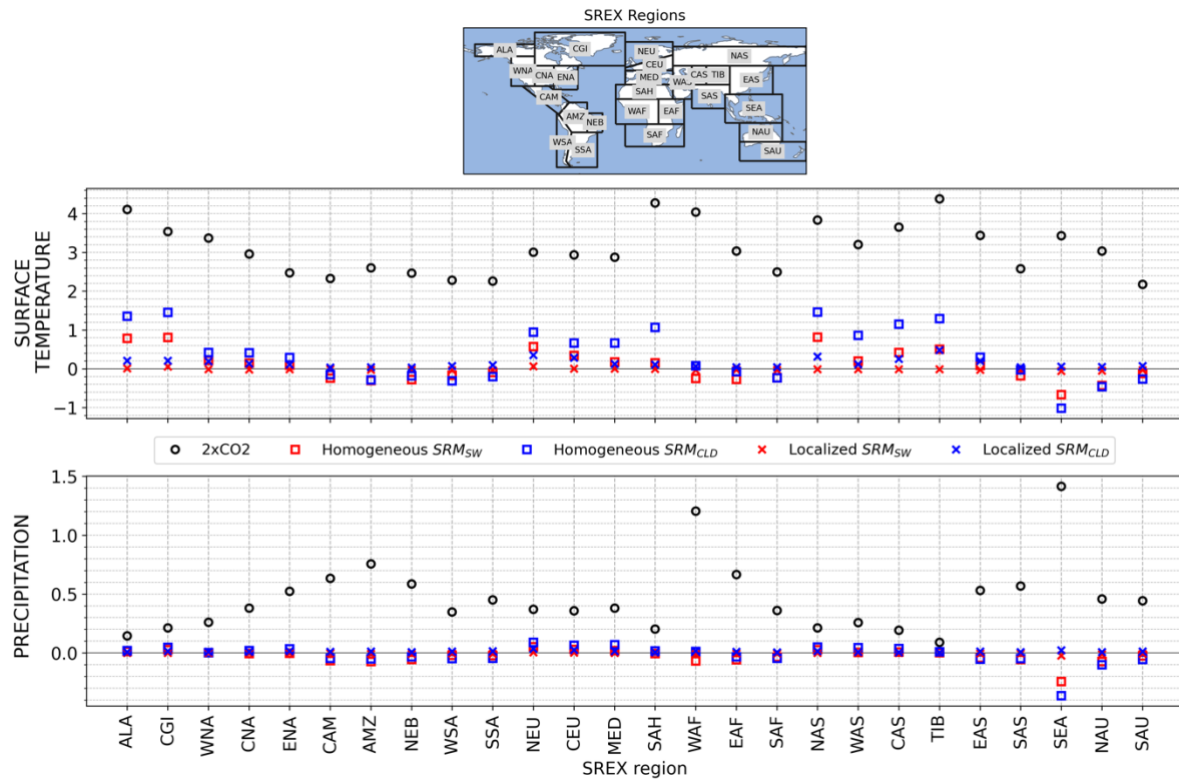
Supplementary Figure 4. Seasonal cycle, computed as $(DJF - JJA)/2$, over SREX regions [Seneviratne et al., 2012], of temperature (upper) and precipitation (lower), for the $2xCO_2$ (black circle), Homogeneous SRM_{SW} (red square), Homogeneous SRM_{CLD} (blue square), Localized SRM_{SW} (red cross) and Localized SRM_{CLD} (blue cross) experiments, respectively.
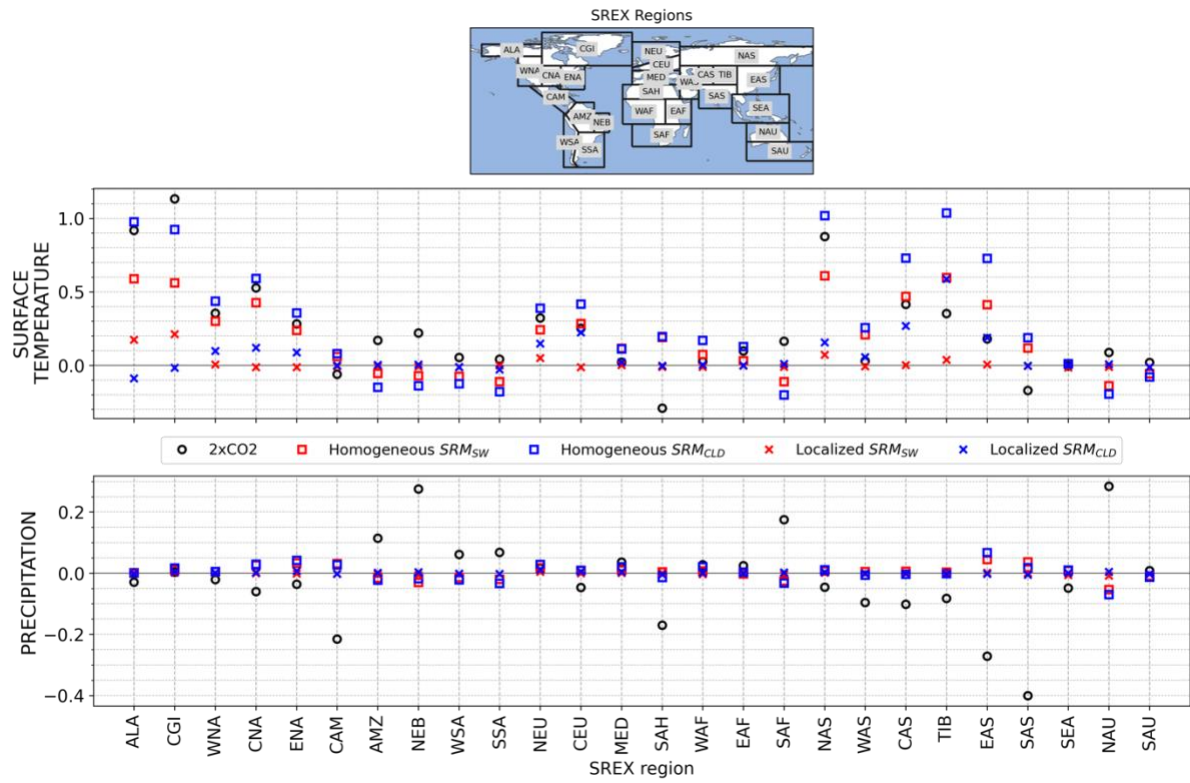
Supplementary Figure 1. Annual mean temperature (upper) and precipitation (lower) anomalies for the 2xCO$_2$ (left), Homogeneous SRM$_{CLD}$ (middle) and Localized SRM$_{CLD}$ experiments (right). The Homogeneous SRM$_{CLD}$ experiment is designed to have the same global mean (gmean) as the control. The area-weighted root mean square (rms) values based on all grid points are shown for each response pattern.

Supplementary Figure 2. Seasonal cycle, computed as $(DJF - JJA)/2$, of temperature (upper) and precipitation (lower) anomalies for the 2xCO$_2$ (left), Homogeneous SRM$_{CLD}$ (middle) and Localized SRM$_{CLD}$ experiments (right). The area- weighted root mean squared (rms) values based on all grid points are shown for each response pattern.

Supplementary Figure 3. Annual mean anomalies over SREX regions [Seneviratne et al., 2012] of temperature (upper) and precipitation (lower), for the 2xCO$_2$ (black circle), Homogeneous SRM$_{SW}$ (red square), Homogeneous SRM$_{CLD}$ (blue square), Localized SRM$_{SW}$ (red cross) and Localized SRM$_{CLD}$ (blue cross) experiments, respectively.

Supplementary Figure 4. Seasonal cycle, computed as $(DJF - JJA)/2$, over SREX regions [Seneviratne et al., 2012], of temperature (upper) and precipitation (lower), for the $2xCO_2$ (black circle), Homogeneous SRM_{SW} (red square), Homogeneous SRM_{CLD} (blue square), Localized SRM_{SW} (red cross) and Localized SRM_{CLD} (blue cross) experiments, respectively.